AD NUMBER

AD031410

NEW LIMITATION CHANGE

TO

Approved for public release, distribution unlimited

FROM

Distribution authorized to U.S. Gov't. agencies and their contractors; Administrative/Operational Use; APR 1954. Other requests shall be referred to Office of Naval Research, 800 North Quincy Street, Arlington, VA 22217-5660.

AUTHORITY

ONR ltr, 26 Oct 1977

Electrical Engineering Research Laboratory
The University of Texas

Report No. 71

30 April 1954

Synthesis of Radio Signals on Overwater Paths

Prepared Under Office of Naval Research Contract Nonr 375(01)
NR 071 032

ELECTRICAL ENGINEERING RESEARCH LABORATORY

THE UNIVERSITY OF TEXAS

Report No. 71

30 April 1954

SYNTHESIS OF RADIO SIGNALS ON OVERWATER PATHS

by

A. H. LaGrone
A. W. Straiton
H. W. Smith

Prepared Under Office of Naval Research Contract Nonr 375(01)
NR 071 032

TABLE OF CONTENTS

FIGURES

ABSTRACT

The fluctuations of radio signals at microwave frequencies on overwater paths are explained on the basis of a periodic rise and fall of the water level. From this study, it is seen that the variations in the radio signal strength will contain the frequency of the water level cycles and also the second and third harmonics of the water level cycles.

This same model predicts that the crosscorrelation function of the fluctuations of the radio signal at two vertically spaced antennas will drop from unity to zero as the separation distance is changed from zero to one-half of a lobe width of a height-gain interference pattern.

Although the model assumes reflection from a plane surface, the results of the study successfully explain most of the features of the observed fluctuations of the radio signals on two overwater paths.

I. INTRODUCTION

A study of the propagation of microwave radio signals on overwater paths is confused by the absence of a suitable model of the rough water surfaces. Reflection from hemisphere, semi-cylinder and broken mirror type surfaces have been considered, but the results obtained are very unwieldy and the appropriateness of the models for actual sea surfaces is questionable.

Many of the characteristics of the overwater radio signal fluctuations can, however, be explained in terms of a plane reflecting surface which rises and falls periodically. This report investigates some of the effects of this simplified model and compares the results with measured overwater propagation data. The comparison indicates that at small grazing angles the simplified model is adequate to explain a number of measured characteristics.

It is not implied that the plane surface model gives a complete explanation of the radio signal fluctuations. It is felt, however, that the plane surface model does give a very good solution where a large coherent reflected component is present. It is felt, further, that a clear understanding of the plane surface case will be of value in approaching the problem of reflections from rough surfaces.

II. MATHEMATICAL FORMULATION OF TOTAL RADIO SIGNAL EQUATION

It is assumed that the path length is short enough so that straight line propagation may be used and that the effect of the earth's curvature may be neglected. With these assumptions, the phase difference, θ, between the direct and the reflected waves at the receiver can be expressed as accurately as needed by the following equation,

$$\theta = \frac{4\pi h_1 h_2}{\lambda D} - \pi \tag{1}$$

where h_1 = transmitter height in feet.
h_2 = receiver height in feet.
D = path length in feet.
λ = wavelength in feet.

The reflecting surface is assumed to rise and fall sinusoidally with time and the deviation of the reflecting plane from its average value is given by

$$\Delta h = b \sin(\omega t) \tag{2}$$

where b is the maximum displacement of the reflecting plane from its average value, measured in feet.

The height of the receiver and of the transmitter are given by

$$h_1 = h_{1_o} + \Delta h \quad \text{and}$$

$$h_2 = h_{2_o} + \Delta h \quad ,$$

respectively.

The equation for θ must now be expanded to show the changes in h_1 and h_2 which result from the reflecting surface height variations. The equation for θ is[2]

$$\theta = \frac{4\pi}{\lambda D}(h_{1_o} + \Delta h)(h_{2_o} + \Delta h) - \pi \tag{3}$$

$$= \frac{4\pi}{\lambda D}\left[h_{1_o} h_{2_o} + (h_{1_o} + h_{2_o})\Delta h + (\Delta h)^2\right] - \pi \tag{4}$$

If we assume that Δh is small compared to $(h_{1_o} + h_{2_o})$ we can rewrite Equation (4) as follows:

$$\theta = \left[\frac{4\pi}{\lambda D}(h_{1_o} h_{2_o}) - \pi\right] + \left[\frac{4\pi}{\lambda D}(h_{1_o} + h_{2_o})\right] \Delta h \qquad (4)$$

$$= \left[\frac{4\pi}{\lambda D}(h_{1_o} h_{2_o}) - \pi\right] + \left[\frac{4\pi}{\lambda D}(h_{1_o} + h_{2_o})\, b\right] \text{Sin } \omega t \qquad (5)$$

$$= \theta_o + \phi \text{ Sin } \omega t \qquad (6)$$

The equation for the resultant received signal, E, is

$$E = E_o \left(1 + Ke^{j\theta}\right) \qquad (7)$$

where, E_o = electric field strength of the direct ray or free space signal at the receiver.
K = reflection coefficient.

The ratio R of the resultant signal to the direct or free space signal is given by

$$R = (E/E_o) = 1 + Ke^{j\theta} \qquad (8)$$

$$= \left(1 + K^2 + 2K \text{ Cos } \theta\right)^{1/2} \angle \delta \qquad (9)$$

where

$$\delta = \text{arc tan } \frac{K \sin \theta}{1 + K \text{ Cos } \theta} \qquad (10)$$

Since our primary interest is in the fluctuations in the total signal amplitude, we will consider only the scalar magnitude of R in Equation (9) which is,

$$|R| = + \left((1 + K^2) + 2K \text{ Cos } \theta\right)^{1/2} \qquad (11)$$

A binominal series expansion of $|R|$ is,

$$|R| = X^{1/2} + KX^{-1/2}\text{Cos } \theta - \frac{K^2}{2} X^{-3/2}\text{Cos}^2\theta + \frac{K^3}{3} X^{-5/2}\text{Cos}^3\theta$$

$$- \frac{5K^4}{8} X^{-7/2}\text{Cos}^4\theta + \frac{35K^5}{40} X^{-9/2}\text{Cos}^5\theta + \ldots \qquad (12)$$

where $X = (1 + K^2)$.

We can now expand the $\text{Cos}^n\theta$ terms in Equation (12) for n = 1, 2, 3, etc., and collect coefficients of like terms.

$$|R| = A_0 + A_1 \text{ Cos } \theta + A_2 \text{ Cos } 2\theta + A_3 \text{ Cos } 3\theta + \cdots \tag{13}$$

where

$$\left.\begin{aligned} A_0 &= X^{1/2} - \frac{K^2}{4X^{3/2}} - \frac{15K^4}{64X^{7/2}} - \frac{105K^6}{256X^{11/2}} - \cdots \\ A_1 &= \frac{K}{X^{1/2}} + \frac{3K^3}{8X^{5/2}} + \frac{35K^5}{64X^{9/2}} + \frac{1155K^7}{1024X^{13/2}} + \cdots \\ A_2 &= -\frac{K^2}{4X^{3/2}} - \frac{5K^4}{16X^{7/2}} - \frac{315K^6}{512X^{11/2}} - \cdots \\ A_3 &= \frac{K^3}{8X^{5/2}} + \frac{35K^5}{128X^{9/2}} + \frac{693K^7}{1024X^{13/2}} + \cdots \end{aligned}\right\} \tag{14}$$

The Cos nθ terms in Equation (13) can also be expanded as follows:

$$\text{Cos } n\theta = \text{Cos } n(\theta_0 + \phi \text{ Sin } \omega t) \tag{15}$$

$$= \text{Cos } (n\theta_0 + n\phi \text{ Sin } \omega t) \tag{16}$$

$$= \text{Cos } (n\theta_0) \text{ Cos } (n\phi \text{ Sin } \omega t) - \text{Sin } (n\theta_0) \text{ Sin } (n\phi \text{ Sin } \omega t) \tag{17}$$

where

$$\left.\begin{aligned} \text{Cos } (n\phi \text{ Sin } \omega t) &= 1 - \frac{(n\phi \text{ Sin } \omega t)^2}{2!} + \frac{(n\phi \text{ Sin } \omega t)^4}{4!} - \frac{(n\phi \text{ Sin } \omega t)^6}{6!} + \cdots \\ \text{Sin } (n\phi \text{ Sin } \omega t) &= (n\phi \text{ Sin } \omega t) - \frac{(n\phi \text{ Sin } \omega t)^3}{3!} + \frac{(n\phi \text{ Sin } \omega t)^5}{5!} - \frac{(n\phi \text{ Sin } \omega t)^7}{7!} + \cdots \end{aligned}\right\} \tag{18}$$

As a final step in the expansion of $\text{Cos}^n\theta$ in Equation (12), the $\frac{(n\phi \text{ Sin } \omega t)^m}{m!}$ terms, m = 0, 1, 2, 3, etc., in Equations (18) can be expanded; and by collecting the coefficients of like terms, a final expression for |R| is obtained in terms of a fundamental (ωt) and its harmonics, (n ωt), as follows:

$$|R| = B_0 + B_1 \text{ Sin } \omega t + B_2 \text{ Cos } 2\omega t + B_3 \text{ Sin } 3\omega t + B_4 \text{ Cos } 4\omega t + \cdots \tag{19}$$

where

$$
\left.
\begin{aligned}
B_0 &= A_0 + A_1 \phi_{01} \cos\theta_0 + A_2 \phi_{02} \cos 2\theta_0 + A_3 \phi_{03} \cos 3\theta_0 + \cdots \\
B_1 &= -A_1 \phi_{11} \sin\theta_0 - A_2 \phi_{12} \sin 2\theta_0 - A_3 \phi_{13} \sin 3\theta_0 - \cdots \\
B_2 &= A_1 \phi_{21} \cos\theta_0 + A_2 \phi_{22} \cos 2\theta_0 + A_3 \phi_{23} \cos 3\theta_0 + \cdots \\
B_3 &= -A_1 \phi_{31} \sin\theta_0 - A_2 \phi_{32} \sin 2\theta_0 - A_3 \phi_{33} \sin 3\theta_0 - \cdots \\
B_4 &= A_1 \phi_{41} \cos\theta_0 + A_2 \phi_{42} \cos 2\theta_0 + A_3 \phi_{43} \cos 3\theta_0 + \cdots
\end{aligned}
\right\} \quad (20)
$$

and

$$
\left.
\begin{aligned}
\phi_{0n} &= 1 - \frac{(n\phi)^2}{4} + \frac{(n\phi)^4}{64} - \frac{(n\phi)^6}{2340} + \cdots \\
\phi_{1n} &= (n\phi) - \frac{(n\phi)^3}{8} + \frac{(n\phi)^5}{192} - \frac{(n\phi)^7}{9216} + \cdots \\
\phi_{2n} &= \frac{(n\phi)^2}{4} - \frac{(n\phi)^4}{48} + \frac{(n\phi)^6}{1536} - \cdots \\
\phi_{3n} &= \frac{(n\phi)^3}{24} - \frac{(n\phi)^5}{384} + \frac{(n\phi)^7}{1536} - \cdots \\
\phi_{4n} &= \frac{(n\phi)^4}{192} - \frac{(n\phi)^6}{3840} + \cdots \\
\phi_{5n} &= \frac{(n\phi)^5}{1920} - \frac{(n\phi)^7}{46080} + \cdots \\
\phi_{6n} &= \frac{(n\phi)^6}{23040} - \cdots \\
\phi_{7n} &= \frac{(n\phi)^7}{322560} - \cdots
\end{aligned}
\right\} \quad (21)
$$

Equation (19) is the final and desired expression for $|R|$. The terms shown in Equations (20) should be adequate for determining the B coefficients for $K < 1$ and $\phi < \frac{1}{2}$. If $K = 1$ and $\phi > \frac{1}{2}$, more terms may have to be added to the series shown in Equations (14), (20) and (21), depending on the accuracy required and the highest harmonics of interest.

An expression similar to Equation (19) can be obtained for the total relative power received if $|R|^2$ is expressed as the sum of a series of sine and cosine terms obtained through an expansion of $\cos\theta$.

$$|R|^2 = (1 + K^2) + 2K \cos \theta \tag{22}$$

$$|R|^2 = C_o + C_1 \sin \omega t + C_2 \cos 2\omega t + C_3 \sin 3\omega t + C_4 \cos 4\omega t + C_5 \sin 5\omega t + \ldots \tag{23}$$

where

$$\left.\begin{aligned} C_o &= (1 + K^2) + 2K \phi_{01} \cos \theta_o \\ C_1 &= 2K \phi_{11} \sin \theta_o \\ C_2 &= 2K \phi_{21} \cos \theta_o \\ C_3 &= 2K \phi_{31} \sin \theta_o \\ C_4 &= 2K \phi_{41} \cos \theta_o \\ C_5 &= 2K \phi_{51} \sin \theta_o \end{aligned}\right\} \tag{24}$$

and the ϕ functions are as defined in Equation (21) for n = 1.

III. NUMERICAL EXAMPLE

Equations (19) and (23) in the preceding section show the frequency of the reflecting surface height variations and its harmonics appearing in the received radio signal. A numerical example is solved in this section to further emphasize the importance of the surface variation frequency and its harmonics in the total signal.

Equation (11) is used to compute $|R|$ for several values of the parameters θ_o and K. A value of 58° is chosen for ϕ in Equation (6) to correspond to experimental data described later. The frequency of the surface variation is arbitrary.

The solution for $|R|$ in the numerical example is shown in Figures 1, 2 and 3. The amplitude of the principal frequency components in $|R|$ is shown in Figures 4, 5 and 6 as a function of θ_o. The amplitude curves in Figures 4, 5 and 6 were obtained by a Fourier [1] analysis of the $|R|$ curves in Figures 1, 2 and 3. Higher harmonics than the third were found to be small.

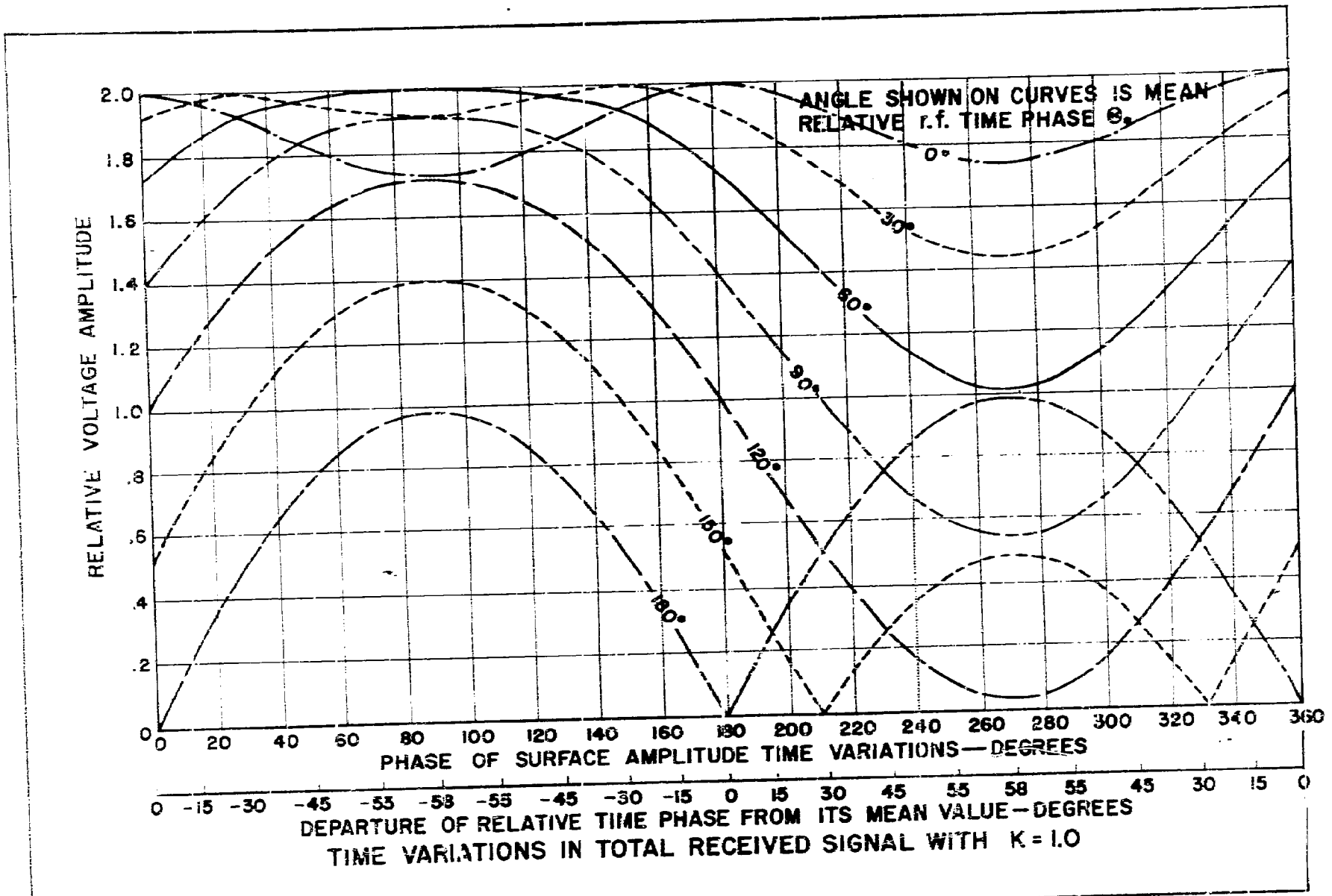
ANGLE SHOWN ON CURVES IS MEAN RELATIVE r.f. TIME PHASE Θ
0°
30°
60°
90°
120°
150°
180°
RELATIVE VOLTAGE AMPLITUDE
2.0
1.8
1.6
1.4
1.2
1.0
.8
.6
.4
.2
0
0 20 40 60 80 100 120 140 160 180 200 220 240 260 280 300 320 340 360
PHASE OF SURFACE AMPLITUDE TIME VARIATIONS—DEGREES
0 -15 -30 -45 -53 -58 -55 -45 -30 -15 0 15 30 45 55 58 55 45 30 15 0
DEPARTURE OF RELATIVE TIME PHASE FROM ITS MEAN VALUE—DEGREES
TIME VARIATIONS IN TOTAL RECEIVED SIGNAL WITH K = 1.0

FIG. 1

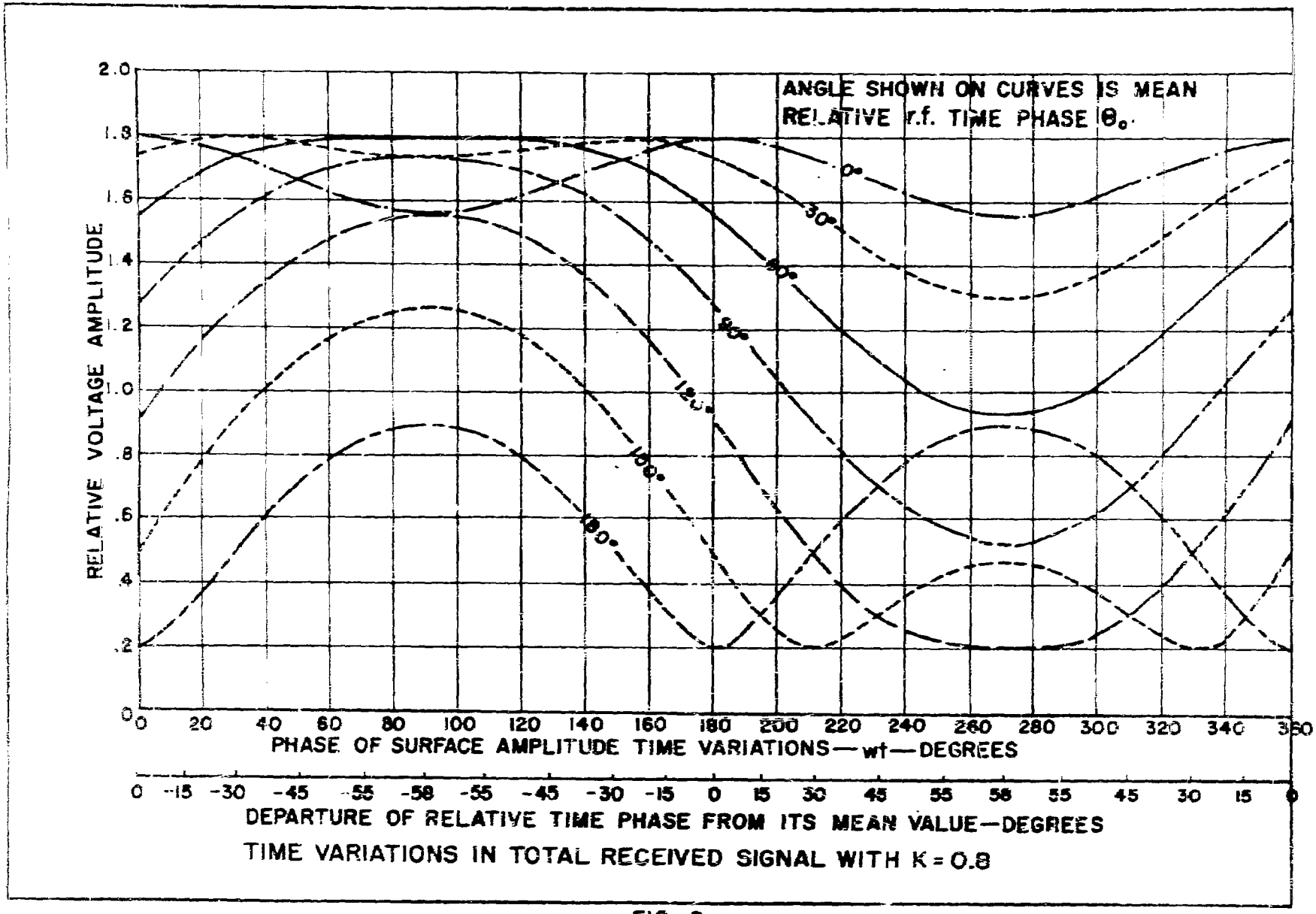
ANGLE SHOWN ON CURVES IS MEAN
RELATIVE r.f. TIME PHASE θ_o.
0°
30°
60°
90°
120°
150°
180°
RELATIVE VOLTAGE AMPLITUDE
2.0
1.8
1.6
1.4
1.2
1.0
.8
.6
.4
.2
0
0 20 40 60 80 100 120 140 160 180 200 220 240 260 280 300 320 340 360
PHASE OF SURFACE AMPLITUDE TIME VARIATIONS—wt—DEGREES
0 -15 -30 -45 -55 -58 -55 -45 -30 -15 0 15 30 45 55 58 55 45 30 15 0
DEPARTURE OF RELATIVE TIME PHASE FROM ITS MEAN VALUE—DEGREES
TIME VARIATIONS IN TOTAL RECEIVED SIGNAL WITH K = 0.8

FIG. 2

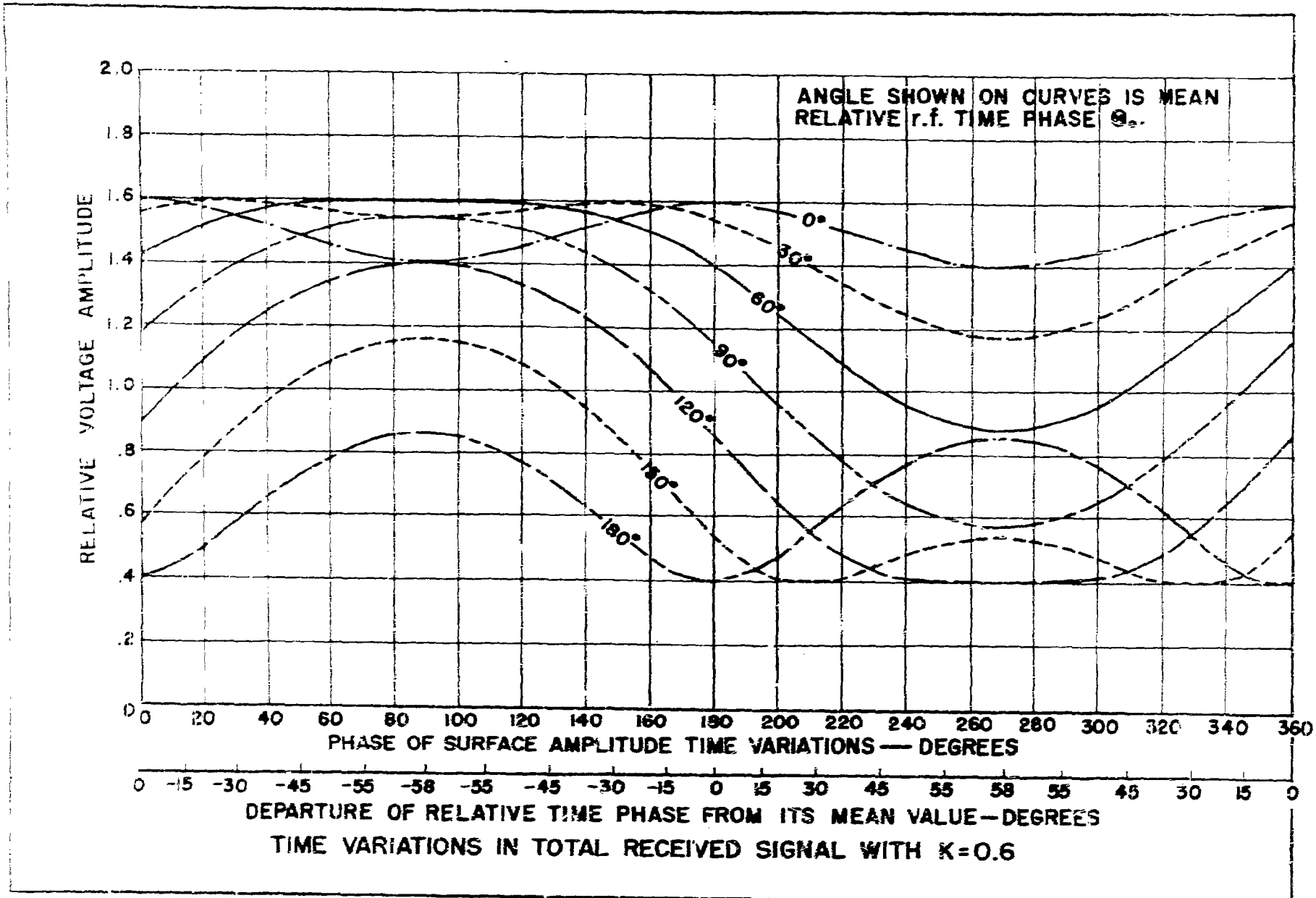
ANGLE SHOWN ON CURVES IS MEAN RELATIVE r.f. TIME PHASE θ_o.
0°
30°
60°
90°
120°
150°
180°
RELATIVE VOLTAGE AMPLITUDE
2.0
1.8
1.6
1.4
1.2
1.0
.8
.6
.4
.2
0
0 20 40 60 80 100 120 140 160 180 200 220 240 260 280 300 320 340 360
PHASE OF SURFACE AMPLITUDE TIME VARIATIONS — DEGREES
0 -15 -30 -45 -55 -58 -55 -45 -30 -15 0 15 30 45 55 58 55 45 30 15 0
DEPARTURE OF RELATIVE TIME PHASE FROM ITS MEAN VALUE—DEGREES
TIME VARIATIONS IN TOTAL RECEIVED SIGNAL WITH K=0.6

FIG. 3

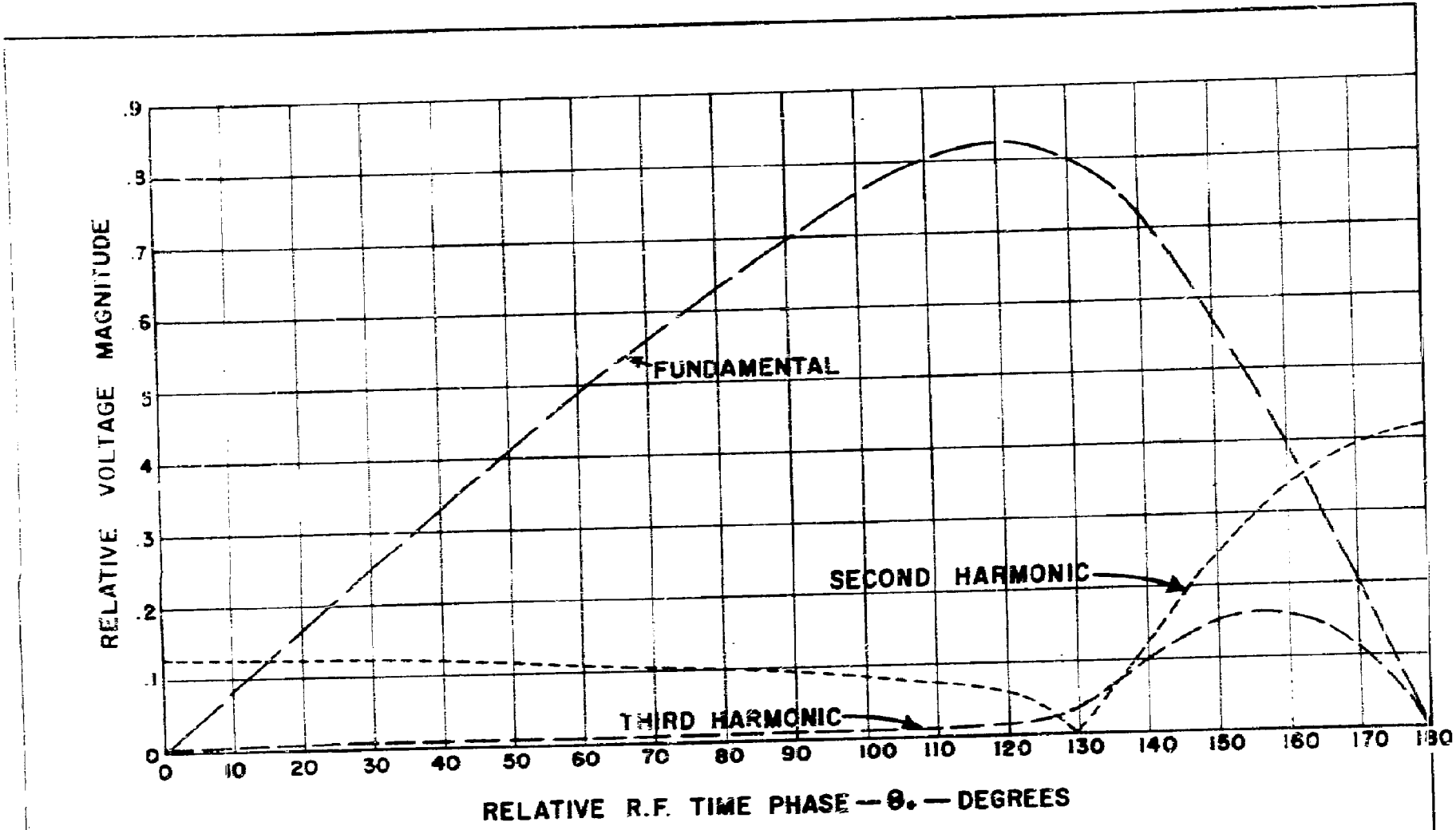

AMPLITUDE DISTRIBUTION OF THE FREQUENCY COMPONENTS IN THE TIME FLUCTUATIONS OF THE RADIO SIGNAL FOR K = 1.0.

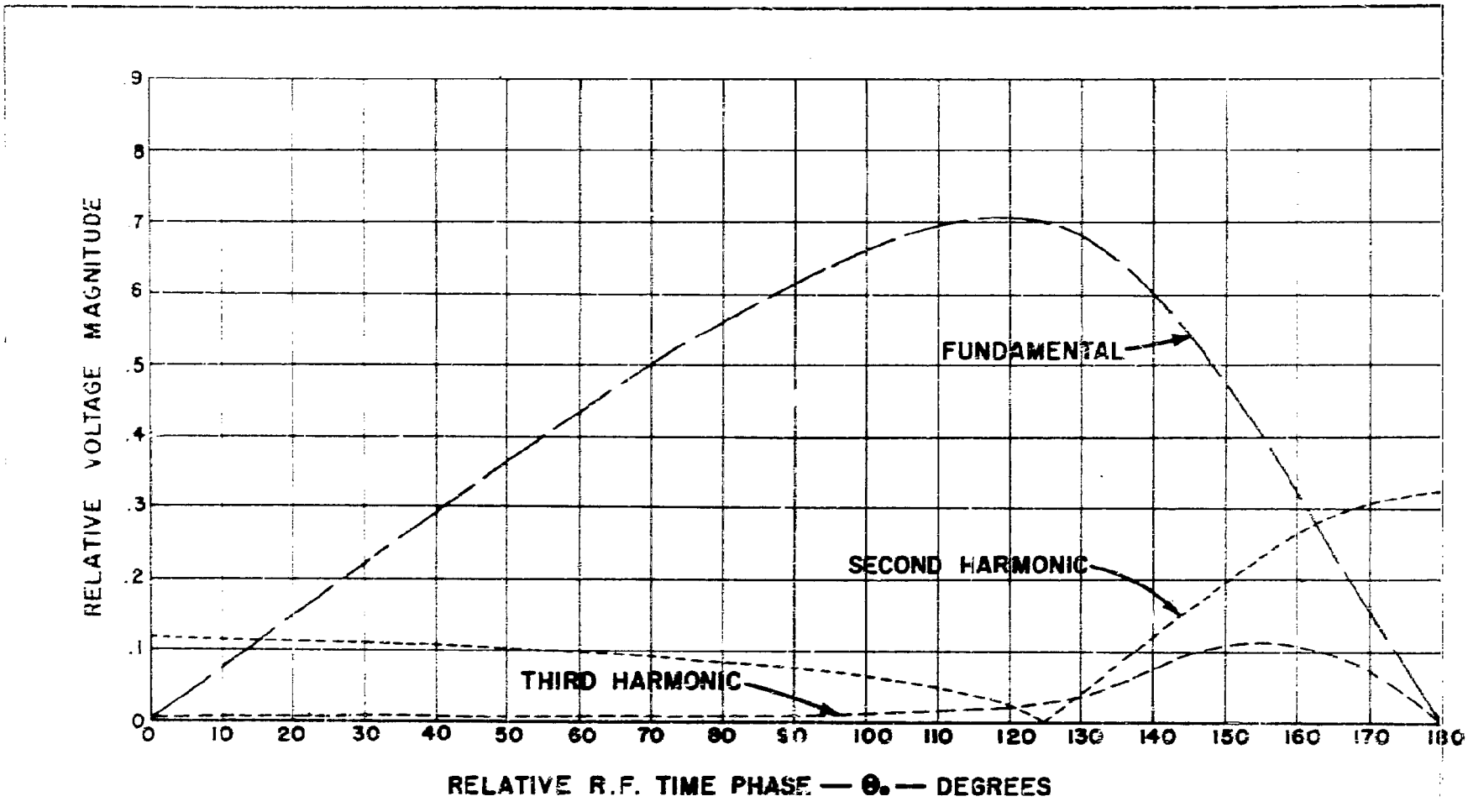

AMPLITUDE DISTRIBUTION OF THE FREQUENCY COMPONENTS IN THE TIME FLUCTUATIONS OF THE RADIO SIGNAL FOR K = 0.8.

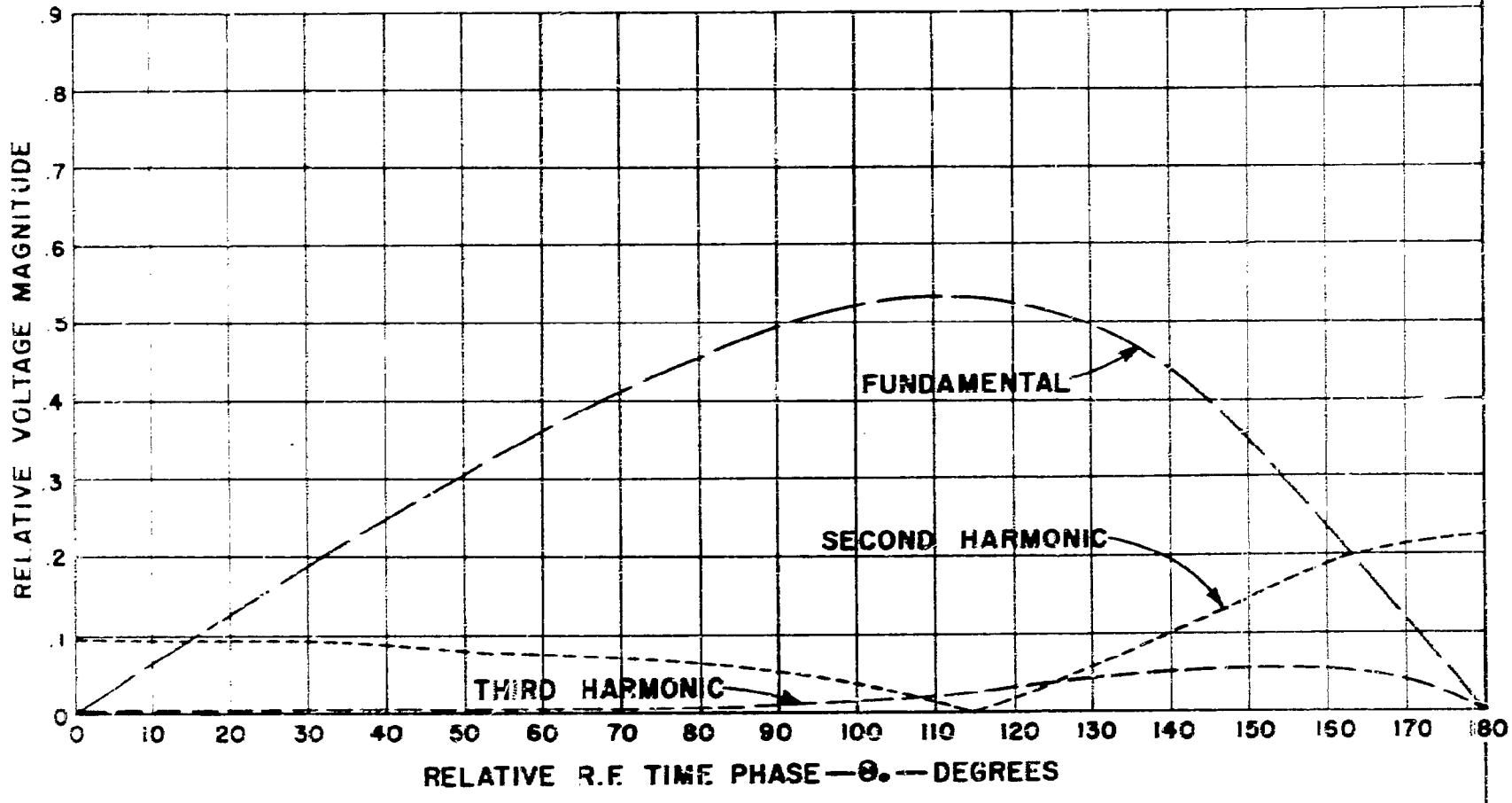

AMPLITUDE DISTRIBUTION OF THE FREQUENCY COMPONENTS IN THE TIME FLUCTUATIONS OF THE RADIO SIGNAL FOR K = 0.6.

The curves in Figures 1 thru 6 graphically show the effect produced by the reflecting surface variation on the radio signal received. The fundamental of the surface variation frequency, for example, is found to be dominant over most of the range of θ_o. A strong second harmonic is found most of the time with a third harmonic becoming prominent for some values of θ_o.

It is important to note that only the even harmonics are present in $|R|$ at $\theta_o = 0^o$ or 180^o, Figures 4, 5 and 6. This would correspond to having the signal fluctuate about a signal maximum or a signal minimum, respectively, in a height-gain curve. The disappearance of the odd harmonics is predicted by Equation (17) since the Sin $(n\theta_o)$ coefficient of Sin $(n\phi \text{Sin } \omega t)$ is zero for $\theta = 0^o$ or 180^o. Thus, this term, which gives the odd harmonics, disappears for these conditions.

The curves in Figure 7 show the magnitude of the three primary frequency components present in the relative radio power received, Equation (24). These curves were computed using the ϕ functions as defined in Equations (21) for $n = 1$.

IV. CORRELATION CONSIDERATION

The normalized crosscorrelation [2] coefficient $\rho_{12}(\tau)$ is computed at $\tau = 0$ for the reflecting surface variation and the fluctuations in the total received signal. The mathematical expression for $\rho_{12}(\tau)$ is

$$\rho_{12}(\tau) = \frac{1}{\overline{y_1(t)}\ \overline{y_2(t)}} \int_{-\pi}^{\pi} y_1(t)\ y_2(t+\tau)\ dt \qquad (25)$$

where $y_1(t) = 1.0 \text{ Sin } \omega t$, (assumed reflecting surface amplitude variation).
$y_2(t)$ = fluctuating part of R [a.c. component of curves in Figures 1, 2 and 3].
$\overline{y_1(t)}$ = effective value of $y_1(t)$
$\overline{y_2(t)}$ = effective value of $y_2(t)$

The crosscorrelation coefficient for $\tau = 0$ is shown in Figure 8 as a function of θ_o for $K = 1.0$. The curves for $K = 0.8$ and 0.6 were also computed but are not shown as there was no significant difference between them and Figure 8.

The crosscorrelation curve in Figure 8 shows a correlation coefficient of zero between the radio signal variations and the reflecting surface variations when $\theta_o = 0^o$ or 180^o, or in terms of height-gain curves, when at a signal maximum or at a signal minimum, respectively.

A single crosscorrelation curve, Figure 9, was computed for the fluctuations in the total signal at $\theta_o = 0^o$ and the fluctuations at other values of θ_o. This was computed for $K = 1.0$ only. The curve shows the correlation to be expected

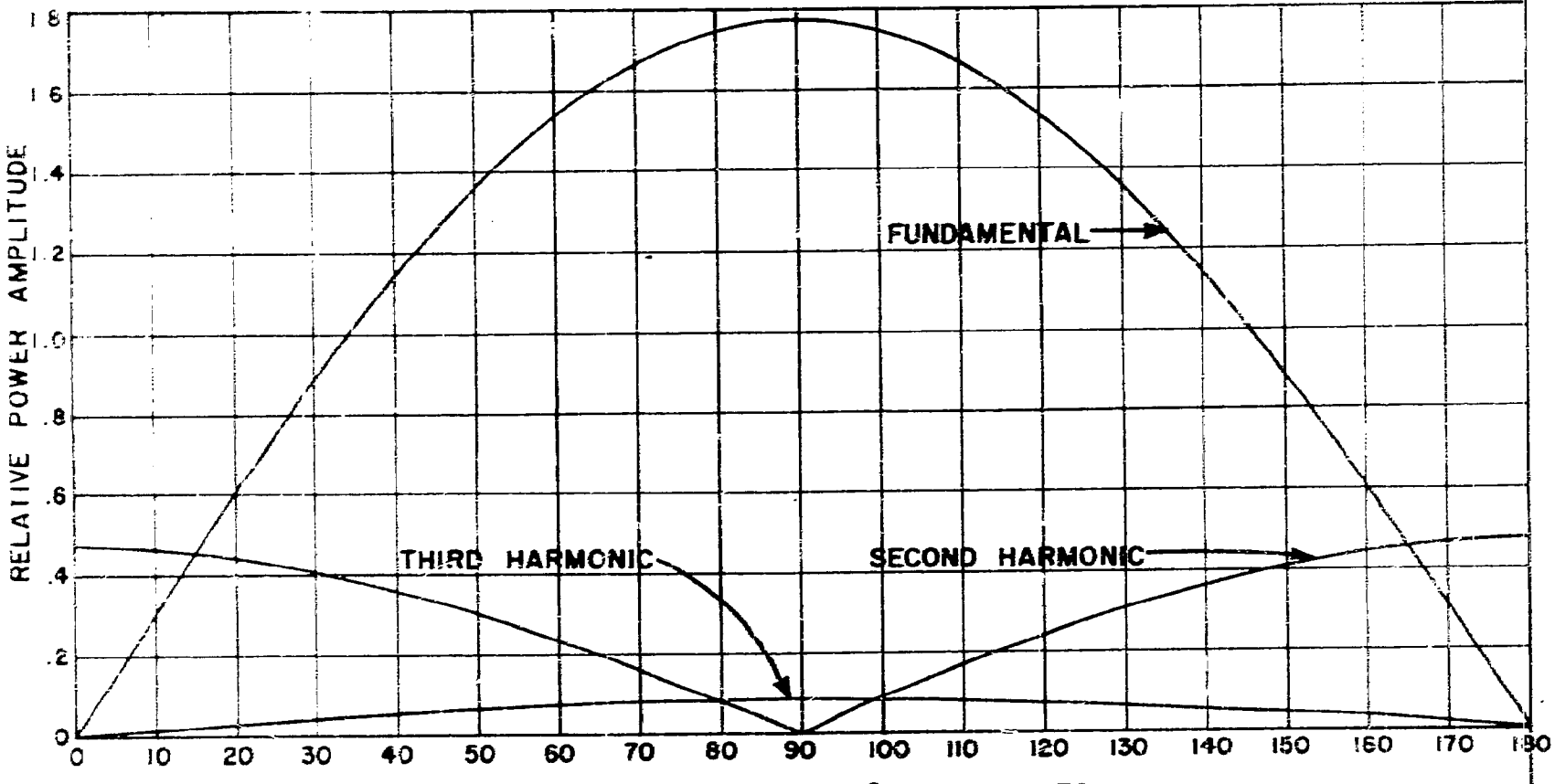

POWER DISTRIBUTION OF THE FREQUENCY COMPONENTS IN THE TIME FLUCTUATIONS OF THE RADIO SIGNAL FOR K=1.0

FIG. 7

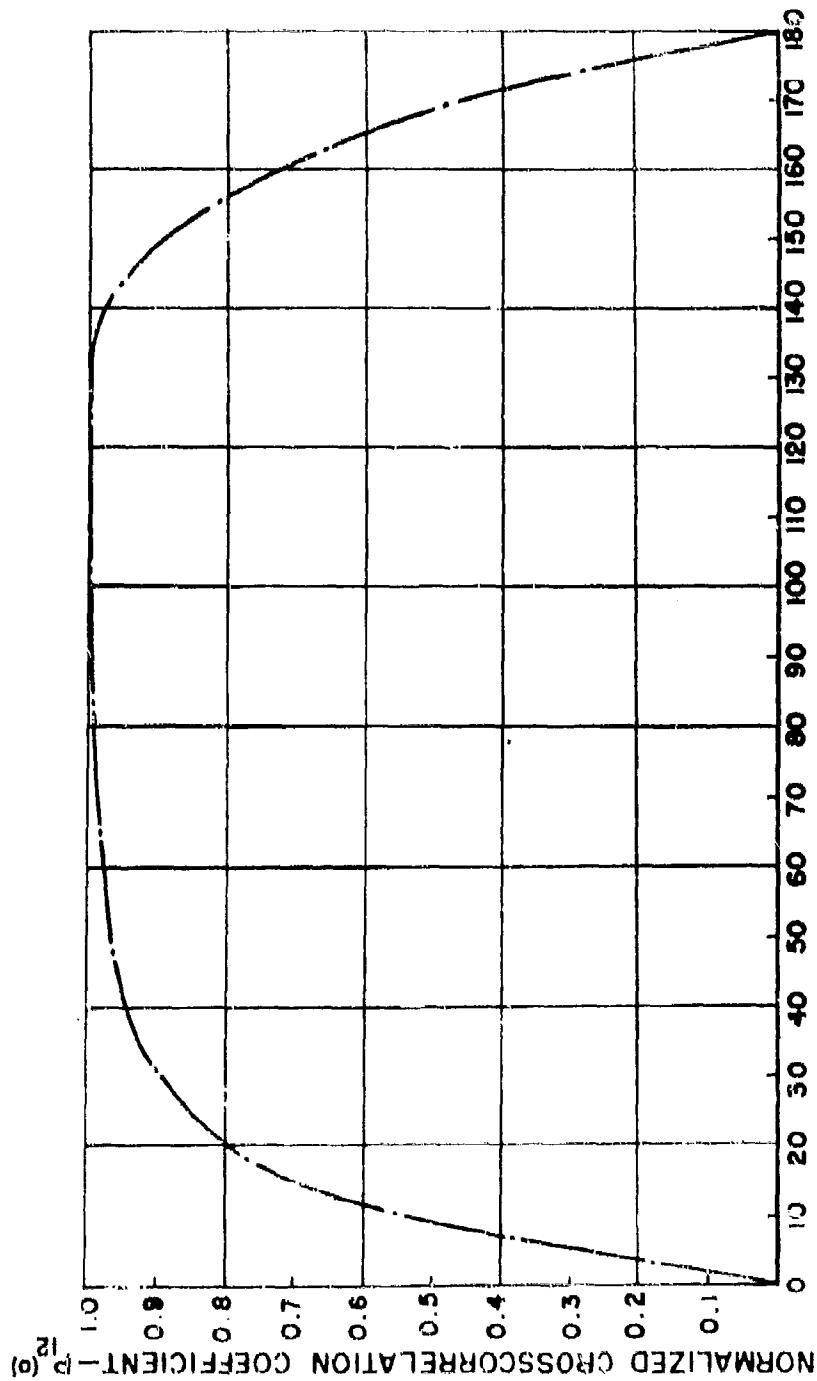

CROSSCORRELATION OF WATER DATA WITH A.C. COMPONENT OF TOTAL RADIO SIGNAL AS A FUNCTION OF RELATIVE TIME PHASE, θ, FOR K=1.0

FIG. 8

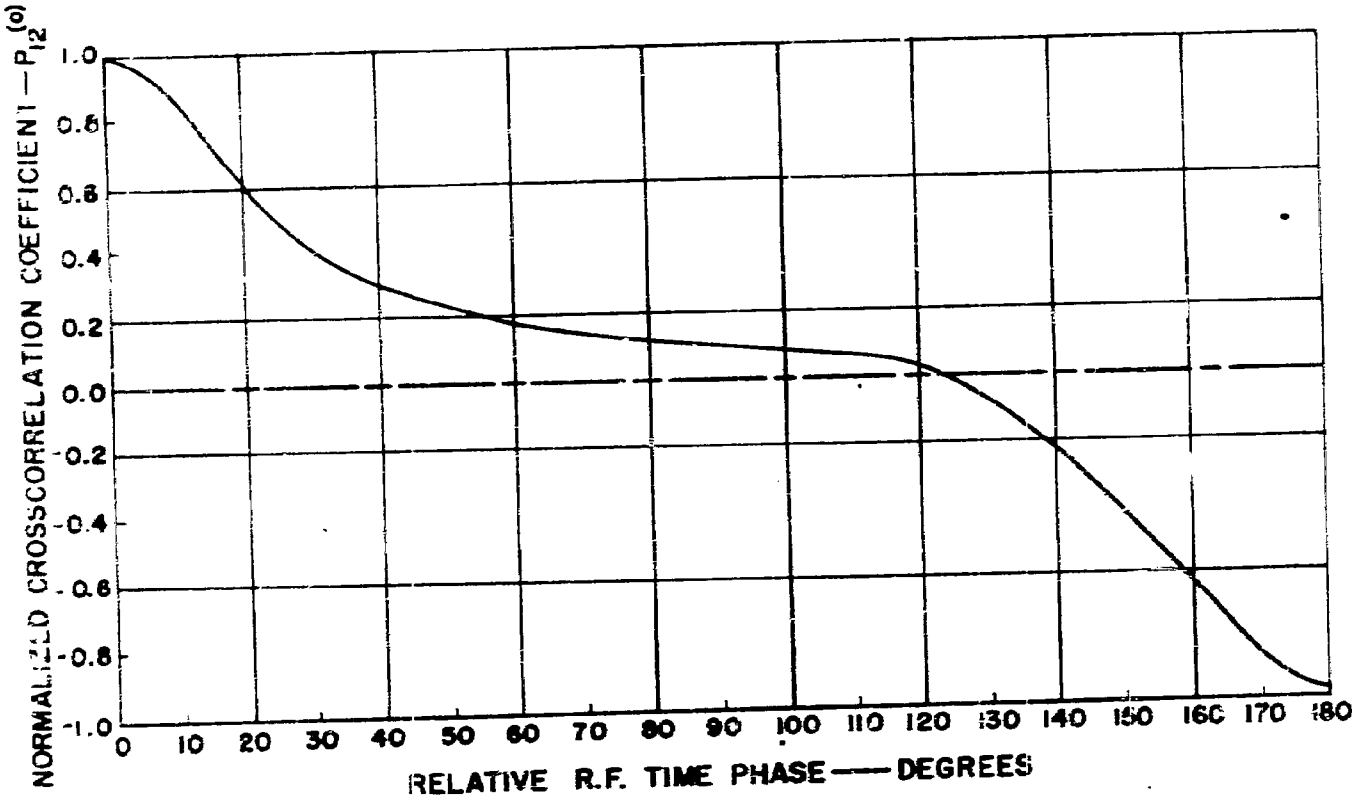

CROSSCORRELATION OF A.C. COMPONENT OF TOTAL RADIO SIGNAL AT $\theta = 0°$ WITH A.C. COMPONENT OF TOTAL RADIO SIGNAL AT OTHER VALUES OF θ, FOR K = 1.0.

FIG. 9

between the fluctuations in the signal at a height-gain maximum and the fluctuations in the signal at other receiver heights which are near the height of the height-gain maximum. This curve, of course, is directly applicable only to the numerical example in this paper.

V. ANALYSIS OF FIELD MEASURED RADIO SIGNALS ON OVERWATER PATH

Signal strength measurements were made on an overwater path, 16,200 feet long, across the Golden Gate Inlet, San Francisco, California, Figure 10. The transmitter height was 87 feet above mean sea level and the receiver height was approximately 50 feet above mean sea level. The water level data [3] were obtained at the pile in Figure 10. A nominal value for the swell amplitudes as measured was two feet, peak to trough.

Spectral density studies [4] were made of the variations with time of the water level and of the variations with time of the radio signal. Sample curves are shown in Figures 11, 12, 13 and 14.

Figure 11 is the water data spectral density curve and is typical of all the water data samples taken. The frequency at which the peak occurred varied slightly from day to day but otherwise the curve remained essentially the same. The spectral density curves of the radio signal varied considerably as Figures 12, 13 and 14 will attest. These are typical cases of the curves found although there were a few cases in which the second peak was larger than the first. There were no cases in which a definite fourth peak was found.

The very good agreement between the central frequency at which the peak occurs in the water spectral density curve, Figure 11, and the central frequency of the first peak in the radio spectral density curves, Figures 12, 13, and 14, suggests very strongly that one results from the other. Also the second and third peaks in the radio data are so near the second and third harmonic frequencies of the first peak central frequency that it must be assumed that they are the harmonics of the first peak central frequency.

The numerical example curves in Figure 7 show how a proper choice of θ_o would yield, by theoretical analysis, curves of $|R|$ having the same fluctuation characteristics as found in the measured data. In Figure 7, for example, a constant amplitude reflected wave with a mean relative time phase of 80° or 100° and a relative time phase variation of 56° Sin ωt would have produced in the total received signal a time varying component having a strong fundamental and a negligible second and third harmonic of the driving frequency as found in the measured data shown in Figure 12. If the mean relative time phase had been 15° or 165°, a spectral density curve similar to the measured curve in Figure 13 would have been obtained. Similarly, a mean relative time phase of 130° would have resulted in the spectral density curve in Figure 14.

The theoretical analysis, of course, is for a single water wave frequency and thus gives only line spectra, whereas, the field measured curves are for conditions of continuous water wave spectra. It is not too difficult, however, to visualize

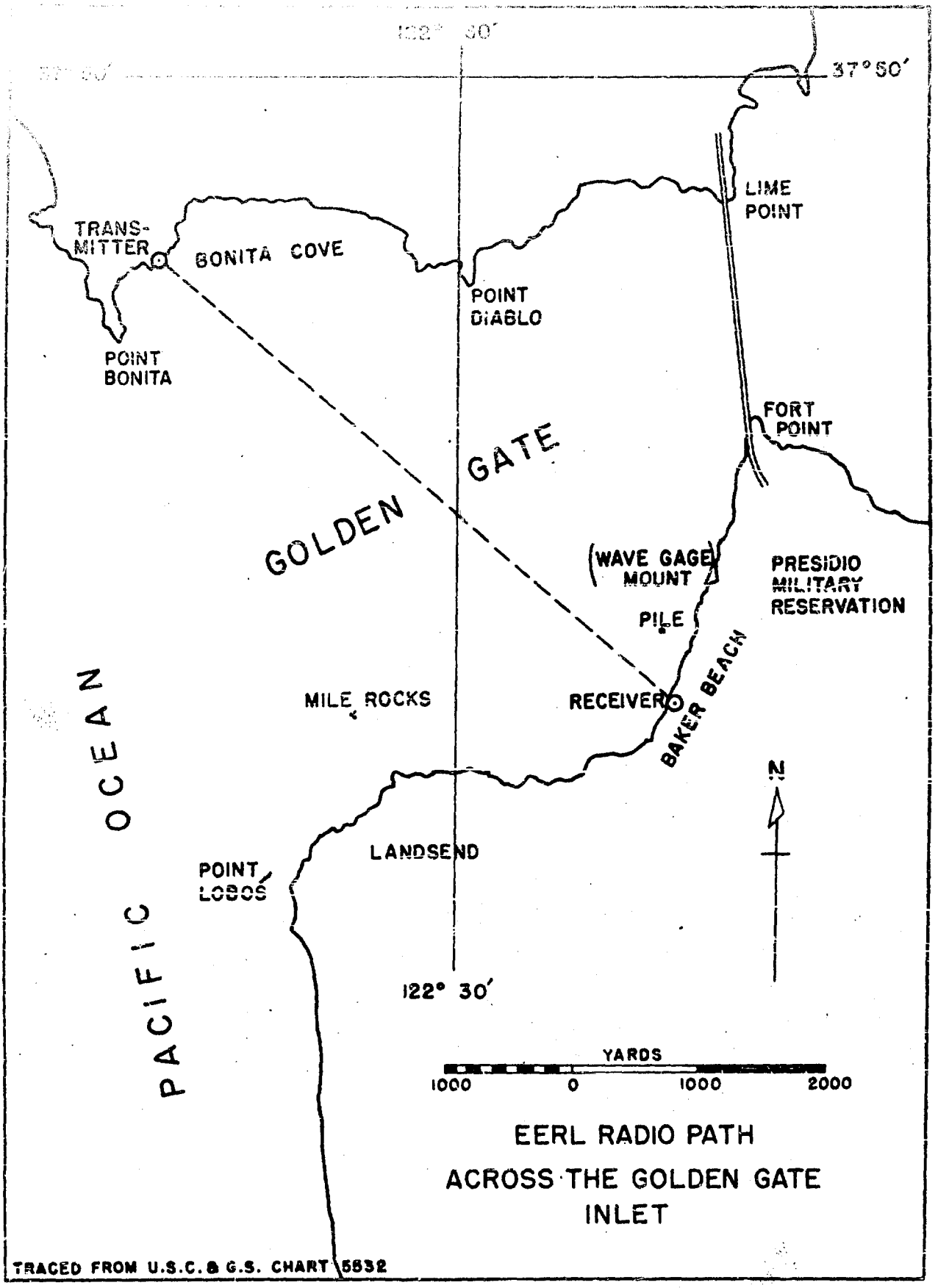
37° 50'
LIME POINT
TRANS-MITTER
BONITA COVE
POINT DIABLO
POINT BONITA
FORT POINT
GOLDEN GATE
WAVE GAGE MOUNT
PRESIDIO MILITARY RESERVATION
PILE
BAKER BEACH
MILE ROCKS
RECEIVER
PACIFIC OCEAN
N
LANDSEND
POINT LOBOS
122° 30'
YARDS
1000 0 1000 2000
EERL RADIO PATH
ACROSS THE GOLDEN GATE
INLET
TRACED FROM U.S.C.& G.S. CHART 5532

FIG. 10

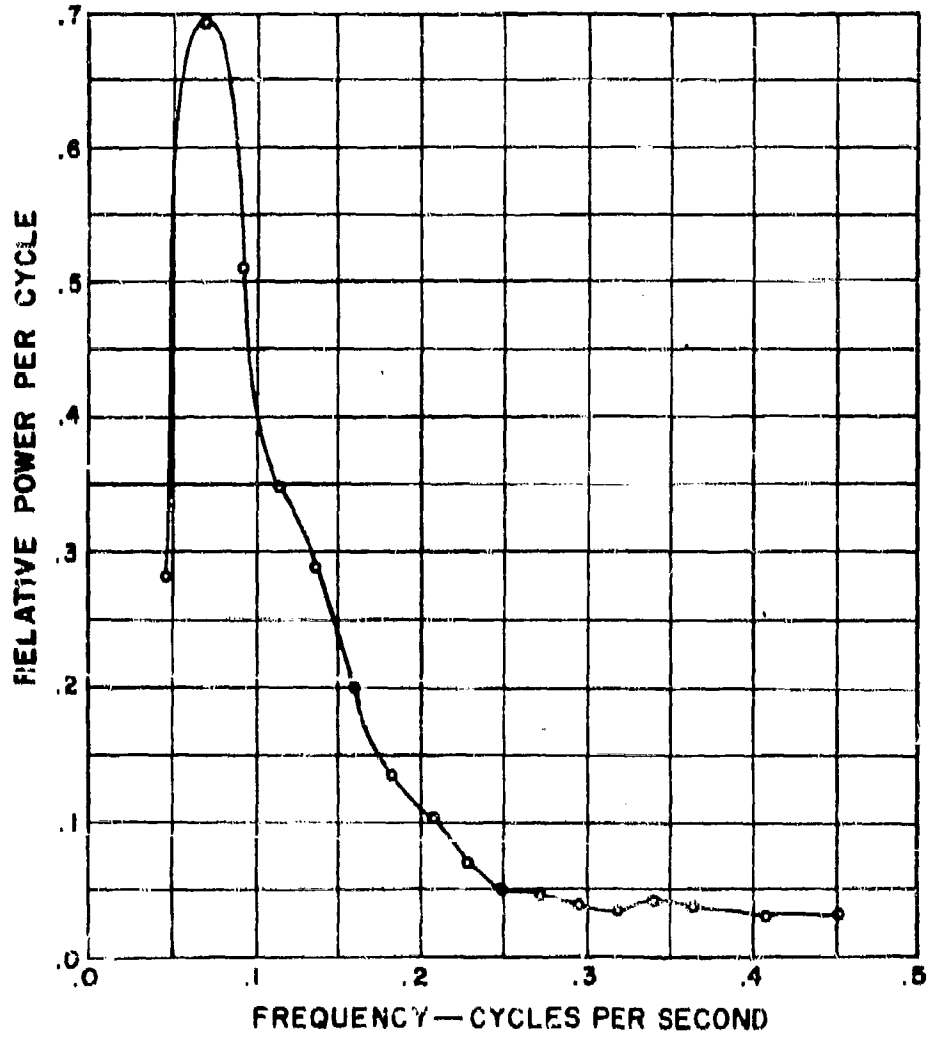

FREQUENCY SPECTRUM OF WATER WAVES.

FIG. 11

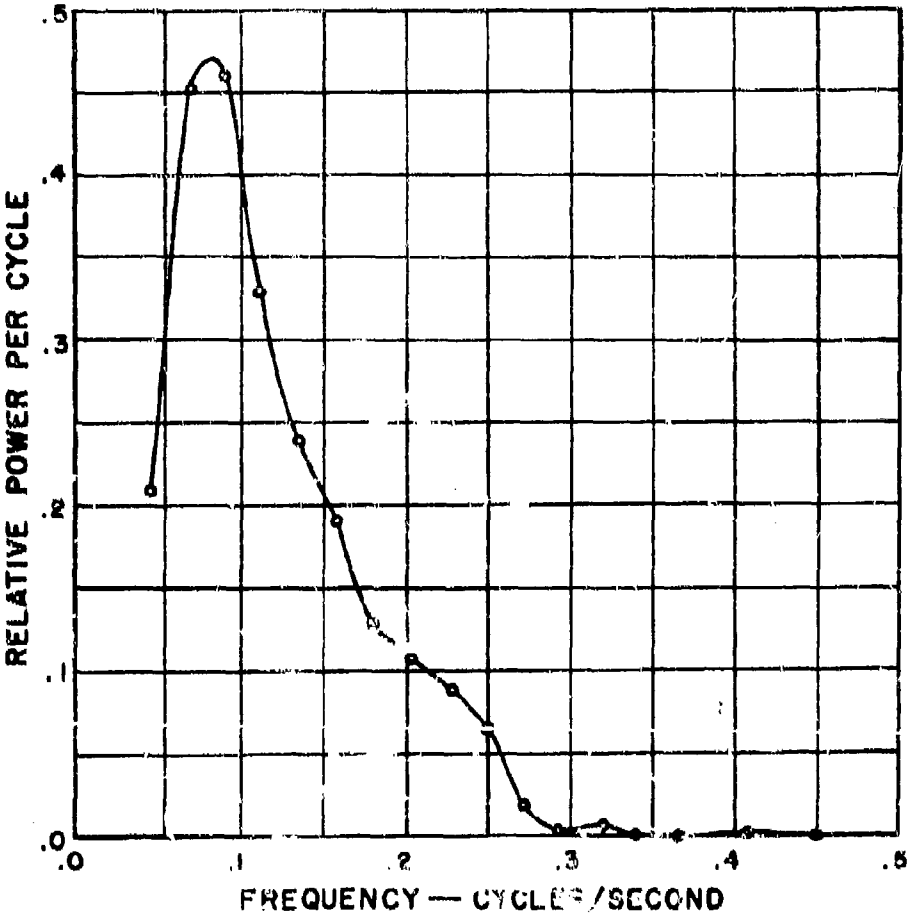

FREQUENCY SPECTRUM OF A.C. COMPONENT OF TOTAL RADIO SIGNAL SHOWING SINGLE PEAK.

FIG. 12

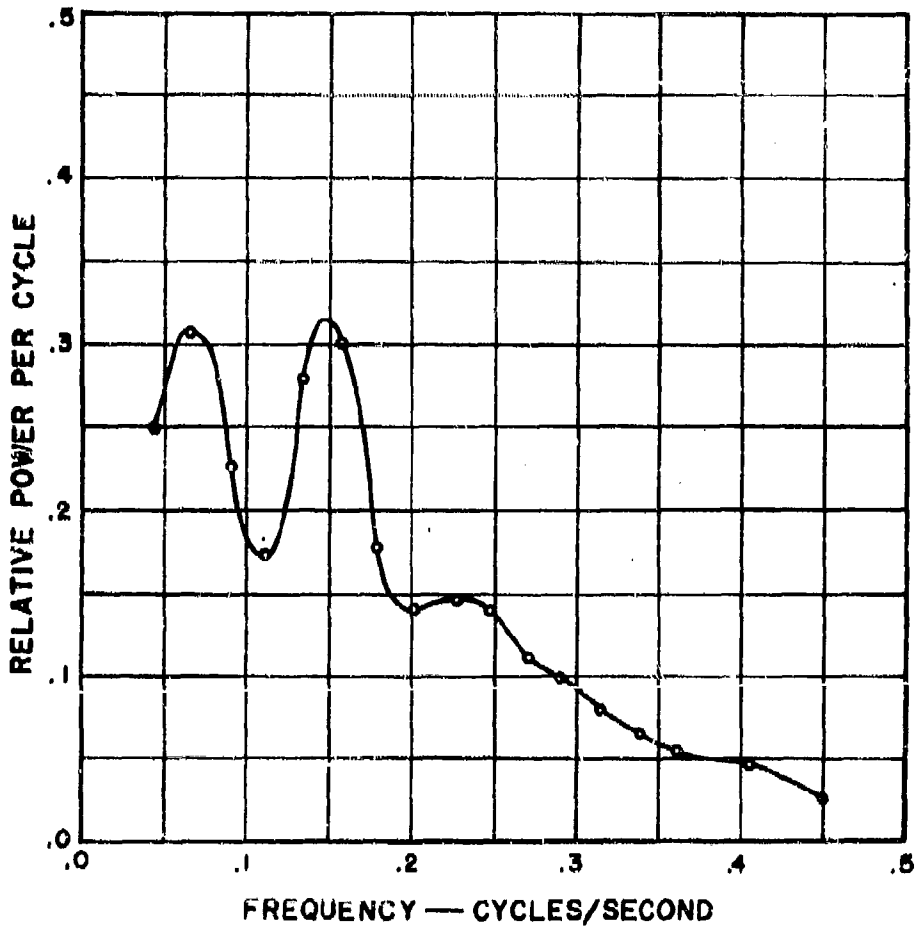

FREQUENCY SPECTRUM OF A.C. COMPONENT OF TOTAL RADIO SIGNAL SHOWING LARGE SECOND HARMONIC.

FIG. 13

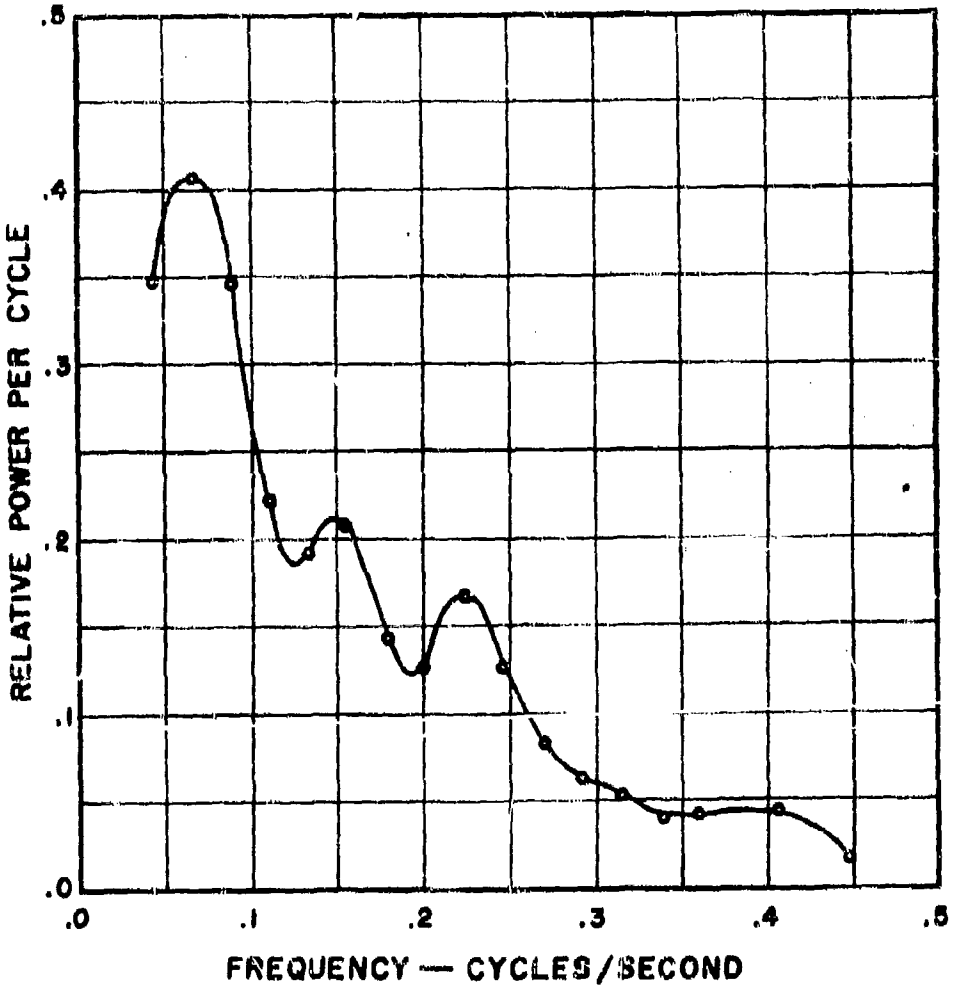

FREQUENCY SPECTRUM OF A.C. COMPONENT OF TOTAL RADIO SIGNAL SHOWING PROMINENT SECOND AND THIRD HARMONICS.

FIG. 14

the driving force in the numerical example as a band of frequencies, in which case, the spectra would be a band spectra similar to the field measured case. Thus we see that the patterns in Figures 12, 13 and 14 plus many others could be obtained from a single specularly reflected wave of constant amplitude.

The mean relative phase θ_0 in the field measured data was essentially constant over short periods of time, however, changes in water level due to the tide did change θ_0 considerably over longer periods of time. Tides varied from four to six feet during the period of measurement and thus changed the effective terminal heights h_1 and h_2 such that θ_0 varied during the day as much as 232° or 348°, depending on the tide that day. This range of variation was sufficient to cover almost all of the possible combinations of components shown in Figure 7.

VI. SYNTHESIS OF RADIO SIGNALS ON AN OVERWATER PATH

The ocean model assumed in Section I is used to compute a height-gain curve for a second overwater path. The equation for the curve is number (8). The components of the relative phase angle θ vary in accordance with Equation (5).

The values assigned the parameters in Equation (8) are those of an overwater path at Barataria Pass, Louisiana [5]. See Figure 15. The values are: $h_1 = 61.7$ feet, $b = 1/12$ foot, $\lambda = 0.105$ foot, and $D = 2780$ feet. The time variations in the height of the reflecting surface are arbitrarily related to the time factor in the height-gain run in such a way that 7.12 cycles of the surface variations are completed in one cycle of the height-gain variation. If we neglect π in the θ_0 component of Equation (5) and assume an initial phase angle for the reflecting surface variations, the equation for θ is

$$\theta = 2.656\, h_2 - \left(\frac{61.7 + h_2}{278.8}\right) \sin (18.9\, h_2 - 3.037) \qquad (26)$$

A value of 0.9 is assumed [5] for K, so that the equation for R is

$$R = 1 + 0.9\, e^{j\left[2.656\, h_2 - \left(\frac{61.7 + h_2}{278.8}\right) \sin (18.9\, h_2 - 3.037)\right]} \qquad (27)$$

Equation (27) is shown plotted in Figure 16(b).

The synthesis of the radio signal is carried one step further in order to investigate the effect on the pattern of the height-gain curve of a small variation in the reflection coefficient. Accordingly, K is assumed to vary in the following manner

$$K = 0.9 - 0.05 \sin (18.9\, h_2 - 3.037) \qquad (28)$$

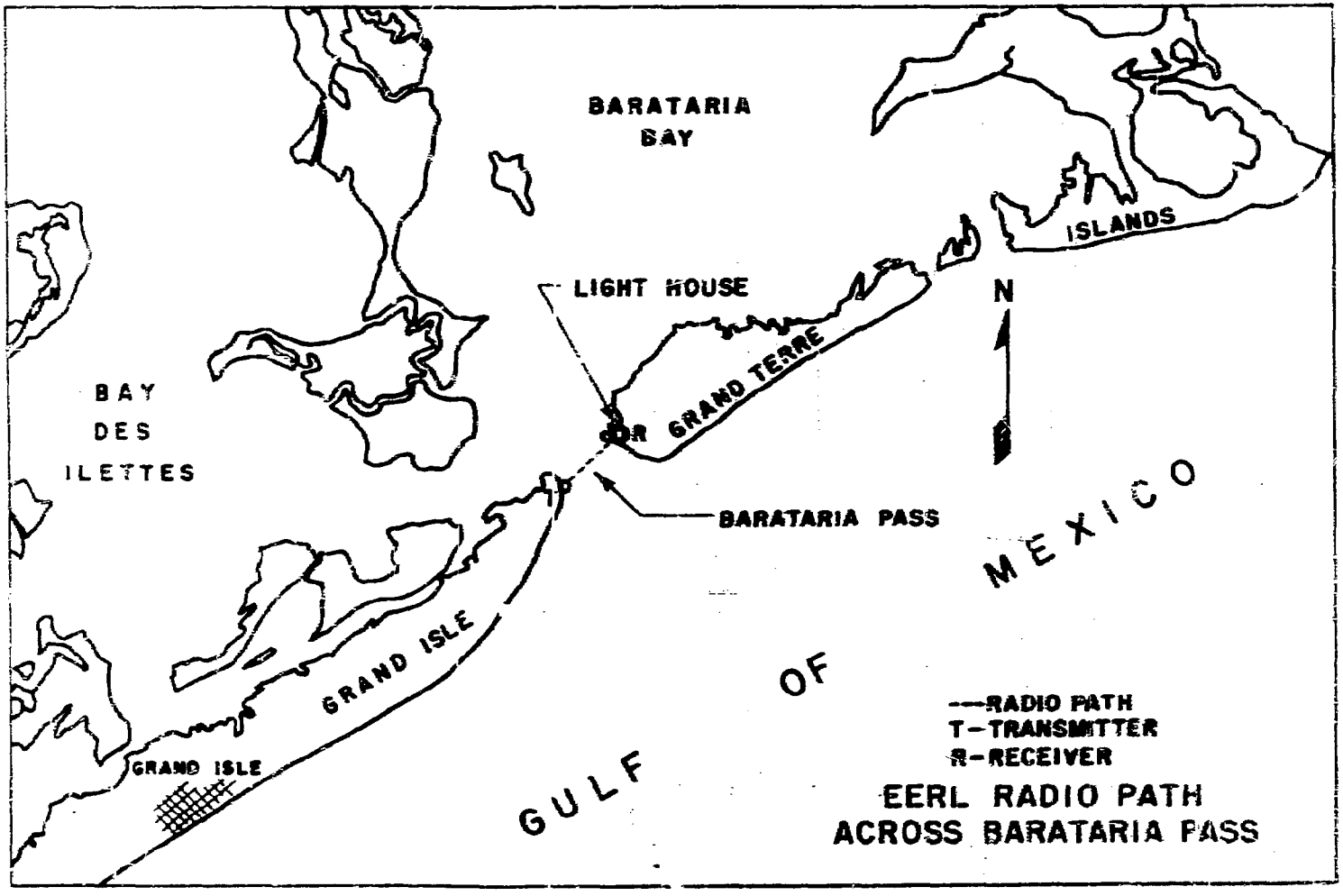
BARATARIA
BAY
ISLANDS
LIGHT HOUSE
N
BAY
DES
ILETTES
GRAND TERRE
BARATARIA PASS
MEXICO
GRAND ISLE
GRAND ISLE
GULF
OF
---RADIO PATH
T-TRANSMITTER
R-RECEIVER
EERL RADIO PATH
ACROSS BARATARIA PASS

FIG. 15

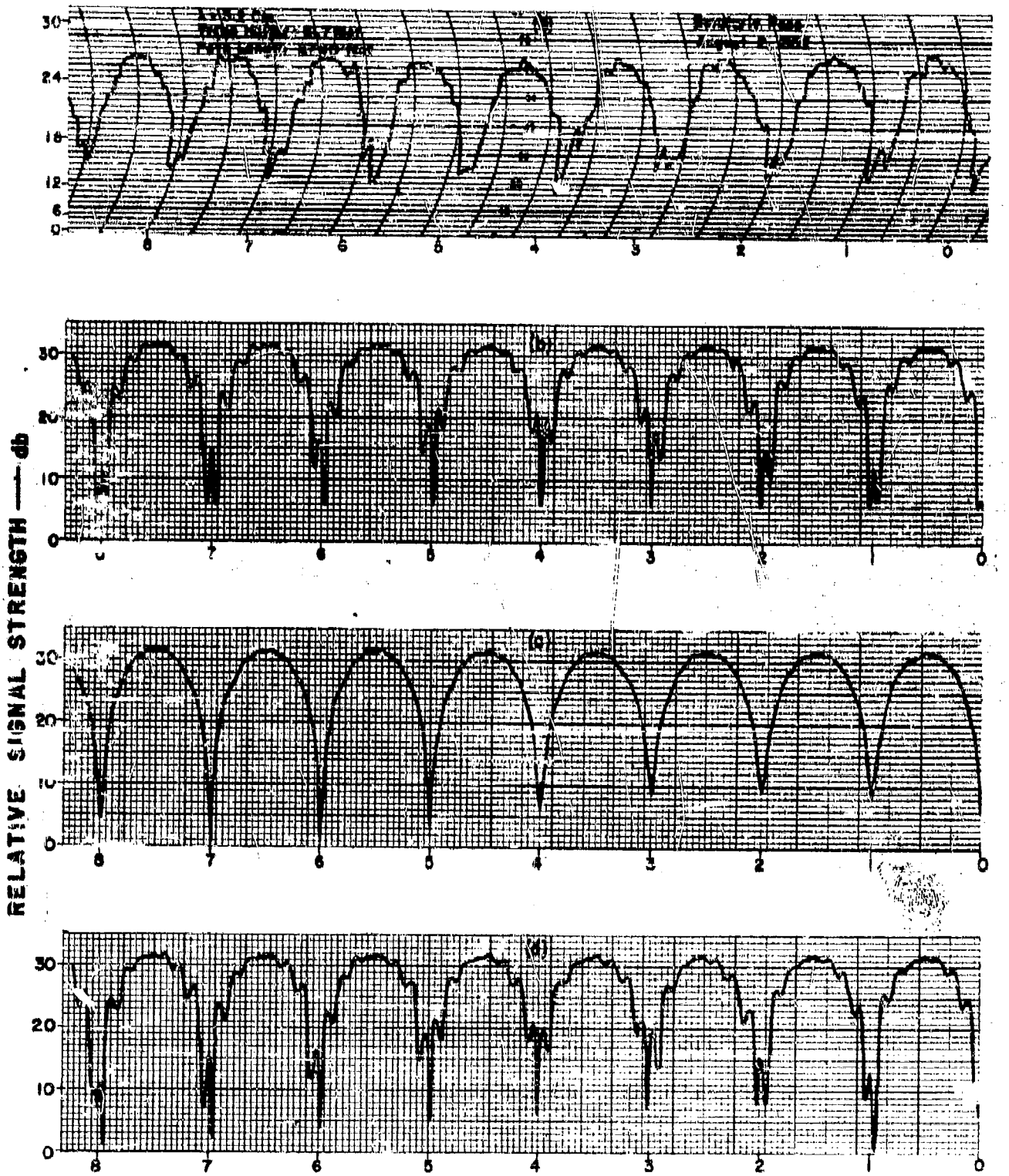

CYCLE – HEIGHT GAIN INTERFERENCE PATTERN

FIELD MEASURED AND THEORETICAL HEIGHT–GAIN CURVES

FIG. 16

If we assume ϕ to be zero, the equation for R is

$$R = 1 + \left[0.9 - 0.05 \sin (18.9\, h_2 - 3.037)\right] e^{j\, 2.656\, h_2} \qquad (29)$$

A plot of Equation (29) is shown in Figure 16(c).

Figure 16(d) is a plot of R with both K and θ having a sinusoidal time varying component. The equation for R is

$$R = 1 + \left(\left[0.9 - 0.05 \sin (18.9\, h_2 - 3.037)\right] e^{j\left[2.65\, h_2 - \frac{61.7 + h_2}{278.8} \sin (18.9\, h_2 - 3.037)\right]} \right) \qquad (30)$$

Figure 16(a) is a sample of the radio signal R as actually measured at Barataria Pass. The agreement of this signal with the synthesized signals in 16(b) and (d) is very good and indicates the extreme importance of the relative phase of the reflected wave.

VII. CONCLUSIONS

1. Variations in the relative time phase of the reflected wave generates, in the combination of the direct wave and the reflected wave in the receiver, a fundamental and higher harmonics of the driving motion causing the phase variations.

2. Normalized crosscorrelation studies of the time variations in the amplitude of a radio signal taken on an overwater path and the associated time variations in the height of the ocean surface may vary from zero to unity, depending on the relative time phase of the reflected radio wave and the direct radio wave.

3. Normalized crosscorrelation studies of the time variations in the amplitude of radio signals taken on vertically spaced antennas may vary from plus or minus one to zero.

4. The good agreement of the spectral density distribution of the time variations in the radio signal with the predicted spectral density distribution based on the assumed ocean model indicates that the assumed model is a good approximation of the true ocean existing at the time the field data were taken.

5. The good agreement referred to in paragraph (4) above also shows very strongly that the relative time phase variations in the reflected radio signal are a major factor in determining the time stability of the amplitude of the total radio signal.

6. The reproducibility of field measured data by relative time phase variations in the reflected ray offers additional evidence of the importance of the relative time phase variations in the time stability of the total radio signal.

7. The prominence of the surface variation fundamental in Figures 12, 13 and 14 suggests that the surface reflected wave comes primarily from a small area around the geometrical image point, i.e., an area of the same order of magnitude as the individual swell wavelength.

BIBLIOGRAPHY

1. "Reference Data for Radio Engineers," Third Edition, American Book - Stratford Press, Inc., p. 291.

2. Jones, Hubert M., et al, "Theory of Servomechanism," McGraw-Hill Book Company, Inc., c. 6.

3. Gerhardt, J. R., "Some Meteorological and Oceanographic Characteristics of the Golden Gate California Area," Electrical Engineering Research Laboratory, The University of Texas, Report No. 3-13, CM-760, to be published soon.

4. Brooks, F. E., H. W. Smith and A. H. LaGrone, Electrical Engineering Research Laboratory, The University of Texas, Report No. 3-14, CM-761, to be published soon.

5. LaGrone, A. H. and C. W. Tolbert, "Reflection Studies of Millimeter and Centimeter Radio Waves for Gulf of Mexico Paths," Electrical Engineering Research Laboratory, The University of Texas, Report No. 64, October, 1952.

DISTRIBUTION LIST

Nonr 375(01) or Nonr-136, P.O.I.

Addressee	Attention, Code	No. of Copies
DEPARTMENT OF THE ARMY		
Engineering & Technical Division Office of the Chief Signal Officer Department of the Army Washington 25, D. C.	SIGOL-2 SIGET	1 1
Director of Research Signal Corps Engineering Laboratories Fort Monmouth, New Jersey		1
DEPARTMENT OF THE NAVY		
Chief of Naval Research Department of the Navy Washington 25, D. C.	Code 427 460 416	2 1 1
Director Naval Research Laboratory Washington 25, D. C.	Code 2000 186-A 3460	6 3 1
Chief, Bureau of Ships Department of the Navy Washington 25, D. C.	Code 810 830-C	1 1
Chief, Bureau of Aeronautics Department of the Navy Washington 25, D. C.	EL 50 EL 90	1 1
Chief, Bureau of Ordnance Department of the Navy Washington 25, D. C.	Re 4[illegible]	1
Chief of Naval Operations Department of the Navy Washington 25, D. C.	Op 2002 Op 55F Op 413	1 1 1
Director Office of Naval Research Branch Office 346 Broadway New York 13, New York		1
Director Office of Naval Research Branch Office The John Crerar Library Bldg. 86 East Randolph Street Chicago, Illinois		2

DEPARTMENT OF THE NAVY (Cont'd)

Director Office of Naval Research Branch Office 1030 E. Green Street Pasadena 1, California		1
Director Office of Naval Research Branch Office 1000 Geary Street San Francisco 9, California		1
Officer-in-Charge Office of Naval Research Navy #100 Fleet Post Office New York, New York		1
Commanding Officer U. S. Naval Underwater Sound Laboratory New London, Connecticut		1
Commanding Officer Naval Air Development Center Johnsville, Pennsylvania	AAEL	1
Director Naval Ordnance Laboratory White Oak, Maryland		1
Commanding Officer U. S. Naval Ordnance Test Station Inyokern China Lake, California		1
Commanding Officer U. S. Naval Postgraduate School Monterey, California	Librarian	1
Director Naval Electronics Laboratory San Diego 52, California	Dr. J. B. Smyth	1

DEPARTMENT OF THE AIR FORCE

Commanding General 3151st Electronics Group Griffiss Air Force Base Rome, New York	ENBPF	1
Commanding Officer Air Force Cambridge Research Center 230 Albany Street Cambridge, Massachusetts		1

DEPARTMENT OF THE AIR FORCE (Cont'd)

Commanding General Headquarters, USAF Washington 25, D. C.	AC-AS/4:AFDRE	1
Commanding General Wright Air Development Center Wright-Patterson Air Force Base Dayton, Ohio	Electronics Subdivision	1
Commander Wright Air Development Center Wright-Patterson Air Force Base, Ohio	Paul W. Springer WCLRD	2

DEPARTMENT OF COMMERCE

U. S. Weather Bureau Department of Commerce Washington, D. C.	Director, Radar Engineering	1
Boulder Laboratories National Bureau of Standards P. O. Box 299 Boulder, Colorado	Radio Division	1
Office of Technical Services Department of Commerce Washington 25, D. C.		1
Director Central Radio Propagation Laboratory National Bureau of Standards Washington 25, D. C.		1

MISCELLANEOUS

Dr. J. E. Boyd Georgia School of Technology Atlanta, Georgia		1
Department of Electrical Engineering University of Michigan Ann Arbor, Michigan	Dr. S. S. Attwood	1
Research Laboratory of Electronics Massachusetts Institute of Technology Cambridge, Massachusetts	H. Zimmerman	1
Federal Communications Commission Pennsylvania Ave. & 12th St., N.W. Washington 25, D. C.	Technical Information Division	1

MISCELLANEOUS (Cont'd)

Department of Electrical Engineering University of California Berkeley 4, California	T. C. McFarland	1
Propagation Laboratory School of Engineering Stanford University Palo Alto, California	Dean F. E. Terman	1
British Commonwealth Scientific Office 1800 K Street, N. W. Washington, D. C.		2
Director Project Hermes General Electric Research Laboratory The Knolls Schenectady, New York		1
Bell Telephone Laboratories Red Bank, New Jersey	H. T. Friis	1
RCA Laboratories Division [illegible] Corporation of America Princeton, New Jersey	Dr. H. H. Beverage	1
Electrical Engineering Research Laboratory University of Illinois Urbana, Illinois	E. C. Jordan	1
Armed Services Technical Information Agency Document Service Center Knott Building Dayton 2, Ohio		5
Cruft Laboratory Room 303A, Pierce Hall Harvard University Cambridge 38, Massachusetts	Mrs. M. L. Cox, Librarian	1
School of Electrical Engineering Cornell University Ithaca, New York	Prof. C. R. Burrows	1
Commandant U. S. Coast Guard Washington 25, D. C.	EEE	1
Project Lincoln, M.I.T. P. O. Box 390 Cambridge 39, Massachusetts	T. J. Carroll	1

MISCELLANEOUS (Cont'd)

Department of Electrical Engineering
California Institute of Technology
Pasadena, California

Dr. C. H. Papas

1